

CFD Simulations of Horizontal Wellbore Cleaning and Cement Placement Processes in Drilling and Completions Applications for Petroleum Engineering

M. Tyagi^{1,2}, M. Zulqarnain¹, D. Yilmaz¹

August 7, 2013

¹CRAFT & HAWKINS DEPARTMENT OF PETROLEUM ENGINEERING

²CENTER FOR COMPUTATION & TECHNOLOGY

LOUISIANA STATE UNIVERSITY

Acknowledgements

- **Students**: Muhammad Zulqarnain, Doguhan Yilmaz
- **Funding**: Turkish National Oil Company, Chevron Emerging Faculty Funds, Gueymard Professorship
- **Computational Resources**: HPC@LSU, Louisiana Optical Network Initiative (LONI), CCT, Petroleum Engineering Department
- **Related Publications**:
 - Zulqarnain, M., Simulations of the Primary Cement Placement in Annular Geometries during Well Completion Using Computational Fluid Dynamics (CFD), LSU MS Thesis (2012).
 - Tyagi, M., Zulqarnain, M., Yilmaz, D., Computational Fluid Dynamics Simulations of Horizontal Wellbore Cleaning and Cement Placement Processes in Drilling and Completions Engineering Applications, Journal of Petroleum Science and Technology, Vol. 2(2), pp. 15-28, 2012.
 - Yilmaz, D., Discrete Phase Simulations of Drilled Cuttings Transport Process in Highly Deviated Wells, LSU MS Thesis (2013).

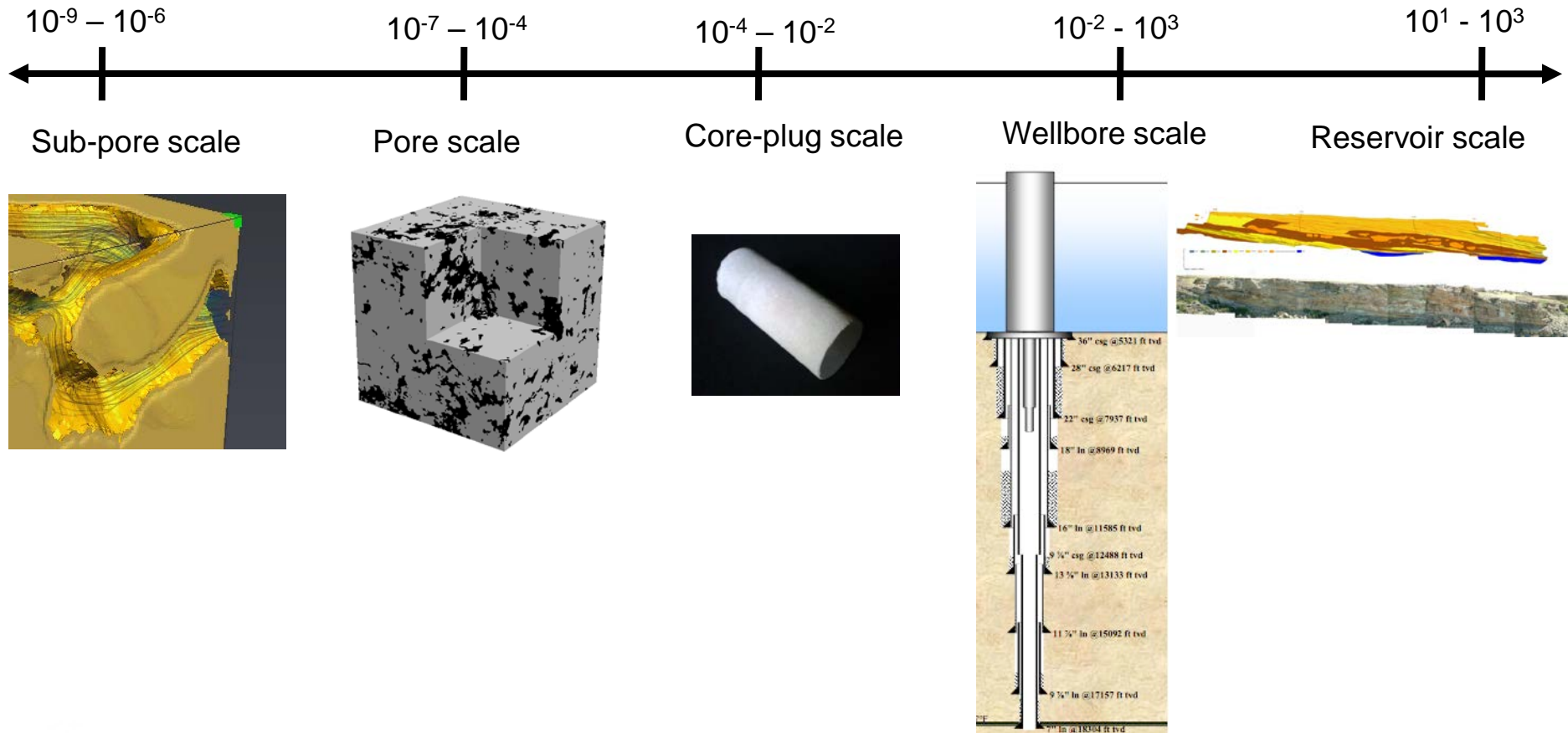


Outline

- Overview: Range of length scales in petroleum engineering applications
- Primary Cement Placement Simulation
 - *Challenges*
 - *Simulation Procedure, V&V*
 - *Parametric Study*
- Cuttings Transport in Deviated Wellbores
 - *Challenges*
 - *Simulation Procedure, V&V*
 - *Parametric Study*
- Concluding Remarks
 - ... and Future Directions



Range of length scales in PETE applications

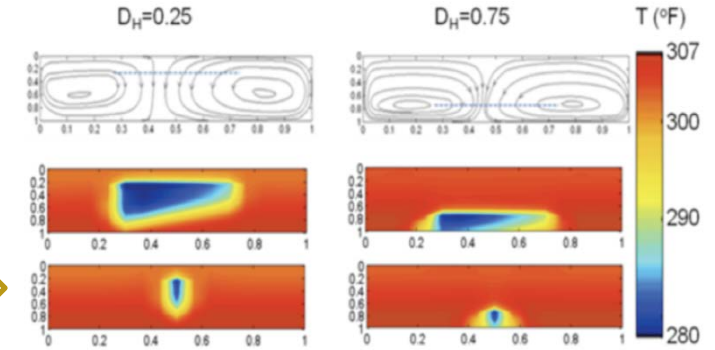
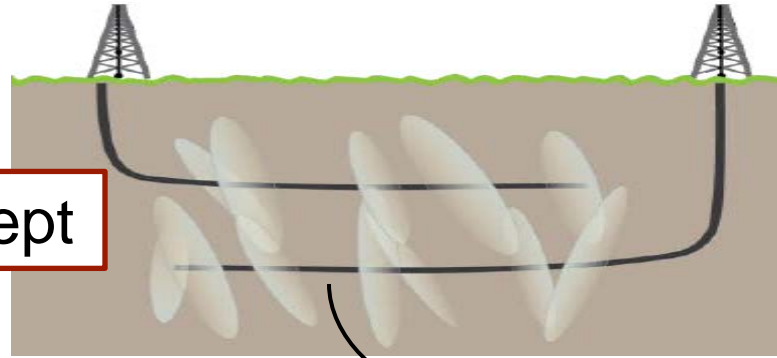


1 Length scale = 1 m

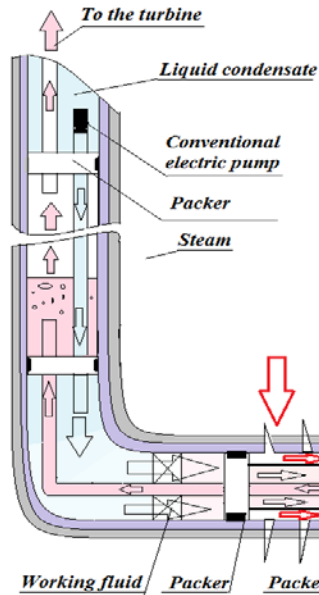
Ref: Deepwater Horizon Accident Investigation Report Appendix W

RELEVANT SCALES FOR FULL WELLBORE GEOTHERMAL RESERVOIR SIMULATION

Concept

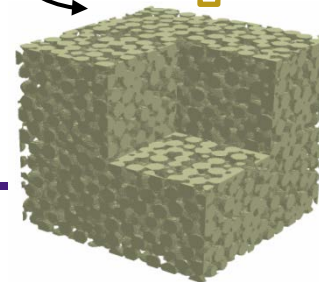
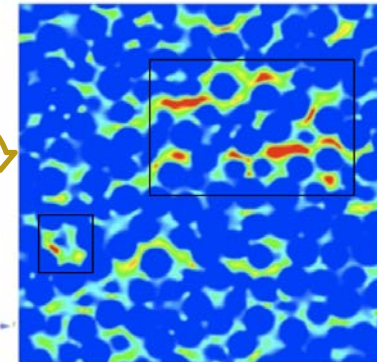


Reservoir Simulation ($\sim 1\text{km}$)



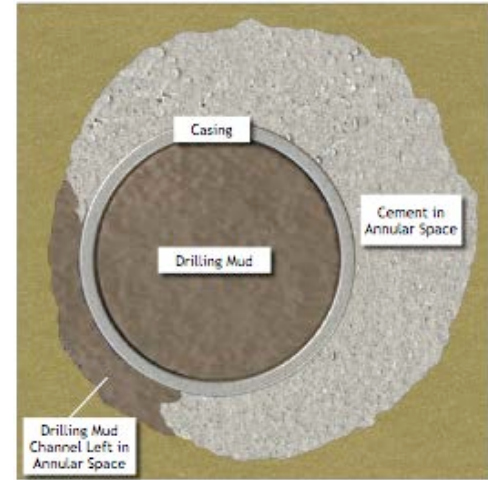
Wellbore CFD Simulation ($\sim 1\text{m}$)

Image-based Porescale Simulation ($\sim 1\mu\text{m}$)



Non-Newtonian Fluid Displacement during Primary Cementing

- ❑ Complete and permanent zonal isolation
- ❑ Complete removal of drilling mud
- ❑ Mud Channels
- ❑ How to remove mud ?
- ❑ Direct contact of mud and cement
- ❑ Spacers

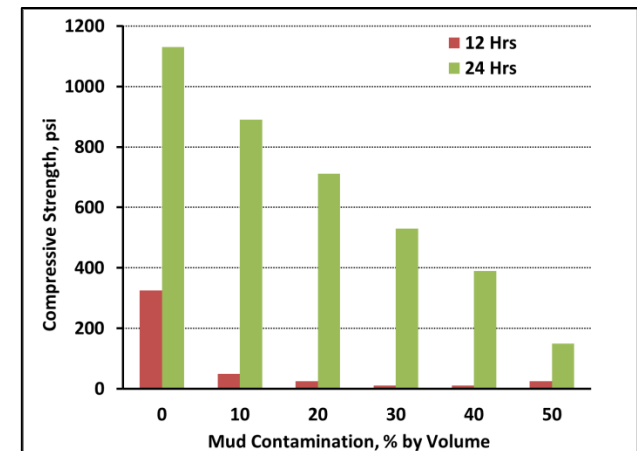


(Top view of an off centered casing*)

*Chief Counsel's Report 02/17/ 2011

Factors affecting cementing job*

- ❑ Mud conditioning
- ❑ Flow rate
- ❑ Casing movement
- ❑ Eccentricity
- ❑ Mud filtration



*Nelson, E.B. Well Cementing, Second Edition.

Data from Abdel-Alim H. El-Sayed, 1995, "Effect of Drilling Mud Contamination on Cement Slurry Properties"

Motivations/Objectives

- ❑ To fill some of the gaps present in terms of quantifications of the whole displacement process.
- ❑ The **root** technical cause of the blowout is now clear*:
 - “The **cement** that BP and Halliburton pumped to the bottom of the well did not seal off hydrocarbons in the formation”.



<http://www.theatlantic.com/technology/archive/2010/10>

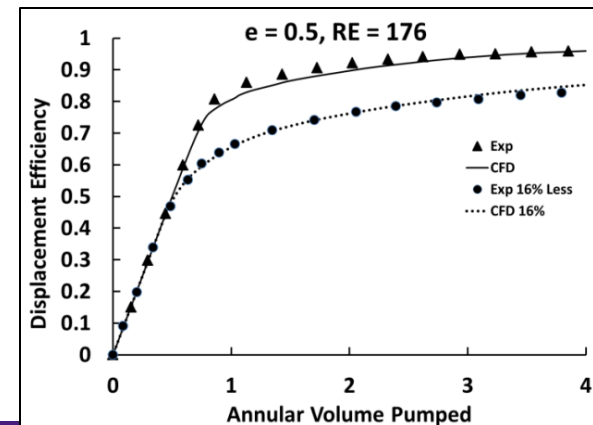
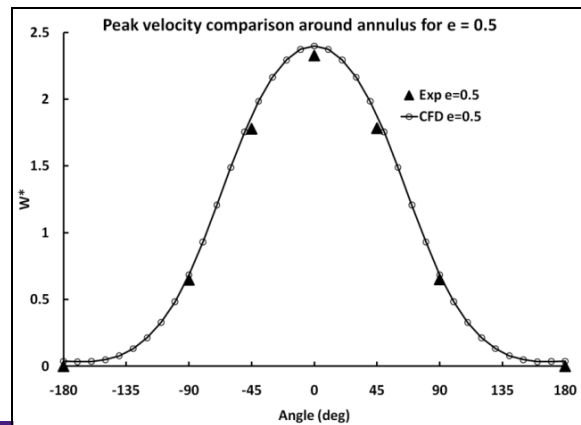
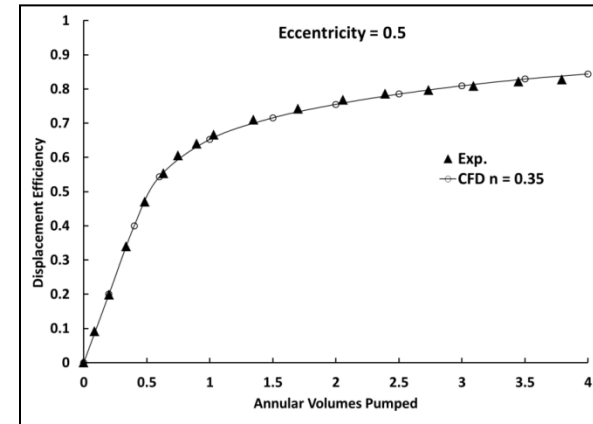
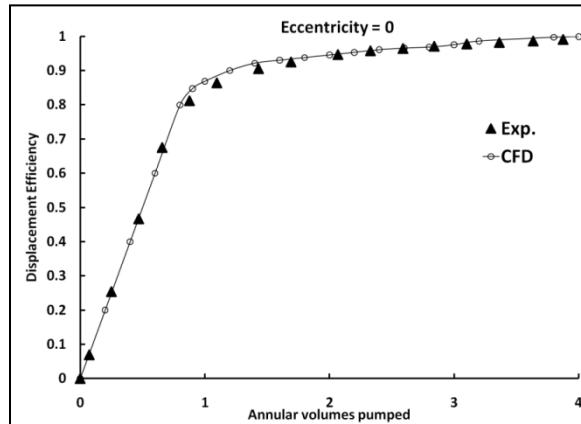
Objective

- ❑ Better understand the complex fluid displacement process and quantification (correlation) of the displacement process in terms of rheological properties of fluids involved under different borehole configurations.



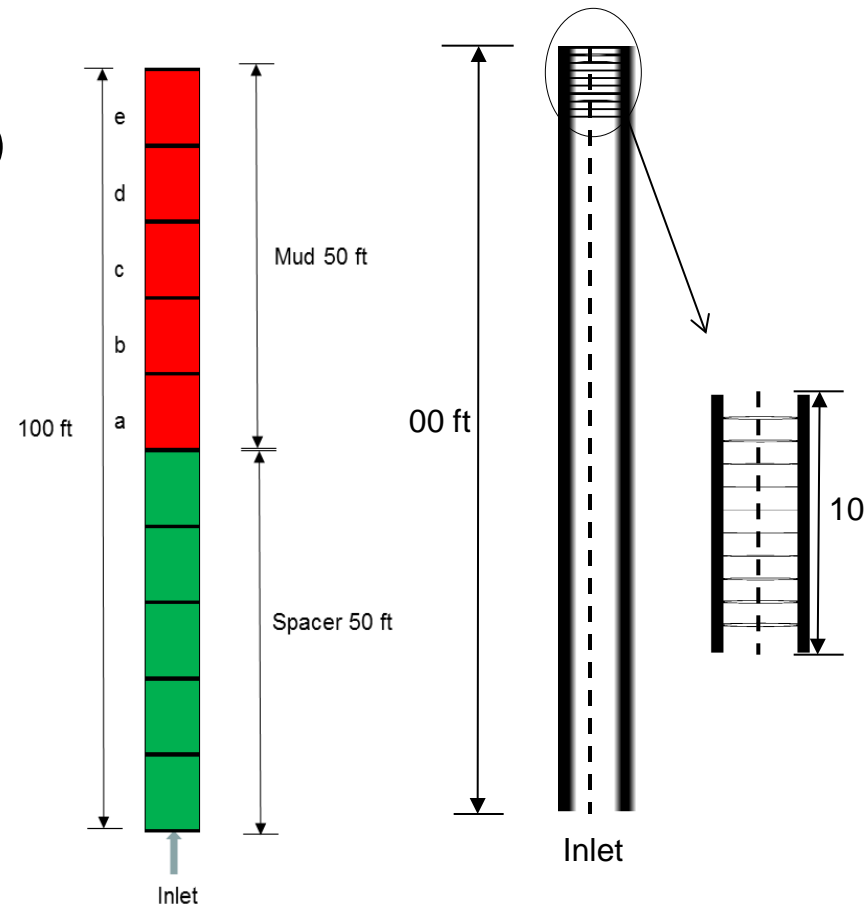
Validation and Verification

Displacement efficiency = (Cement/total volume of channel)



Numerical Setup

- ❑ Computational Fluid Dynamic (CFD)
- ❑ Volume of Fluid (VOF) method¹
- ❑ Interfacial reconstruction scheme²
- ❑ Power Law/ Herschel Bulkley
- ❑ Laminar/ Turbulent flow



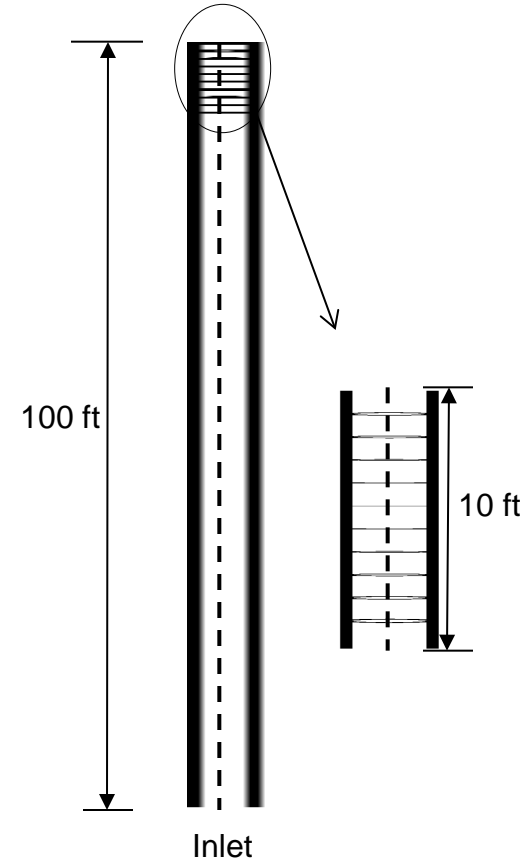
Simulation Setup

- Geometric details are taken from (D.J. Guillot et al. 2007)

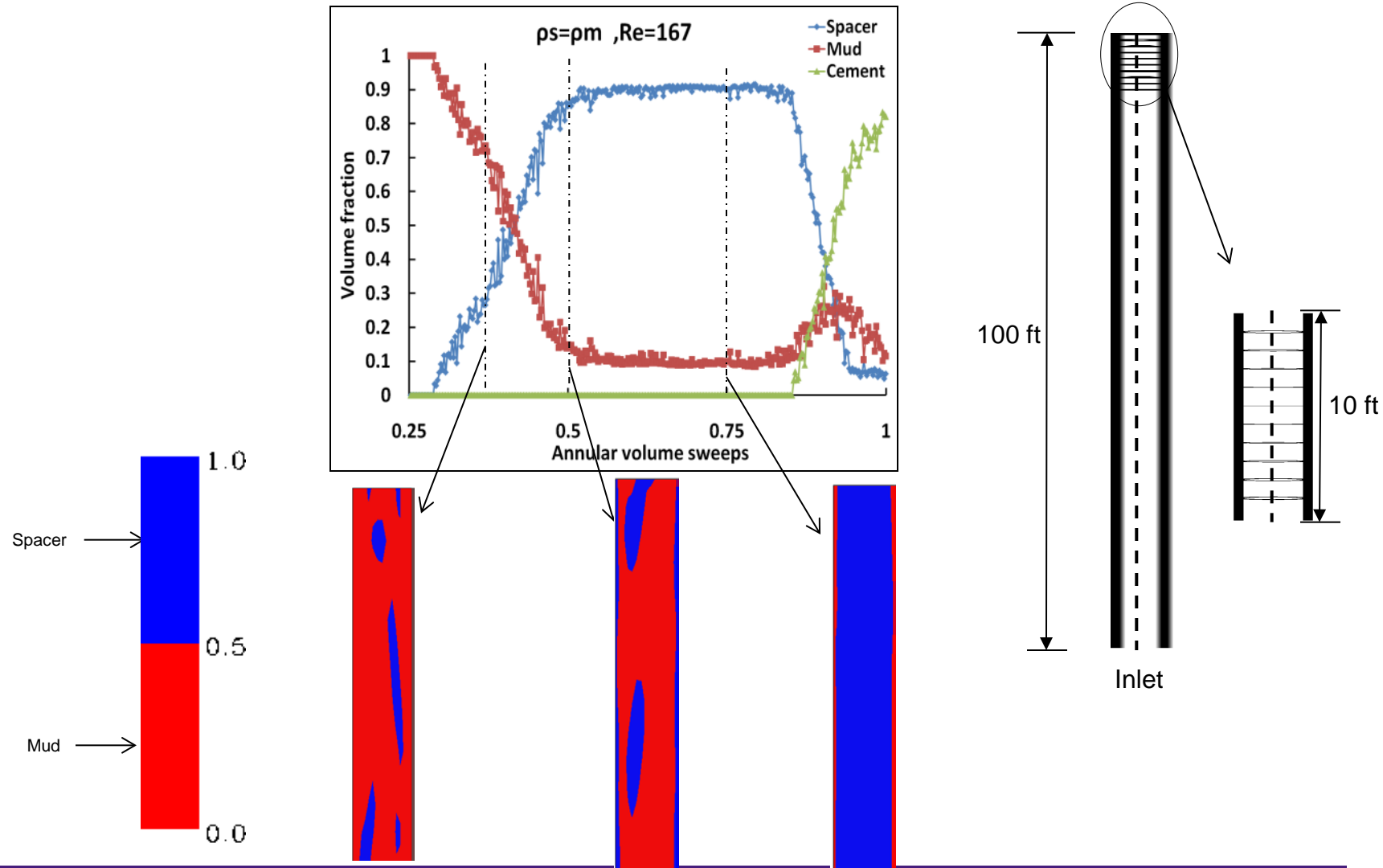
Casing OD (in)	9.675
Open hole dia (in)	12.597
Annular length (ft)	100

- Fluid Properties** (Wilson& Sabins 1988)

	n	K(eq. cp)	ρ(lbm/gal)
Cement	0.308	4708	15.8
Mud	0.607	1346	13.1



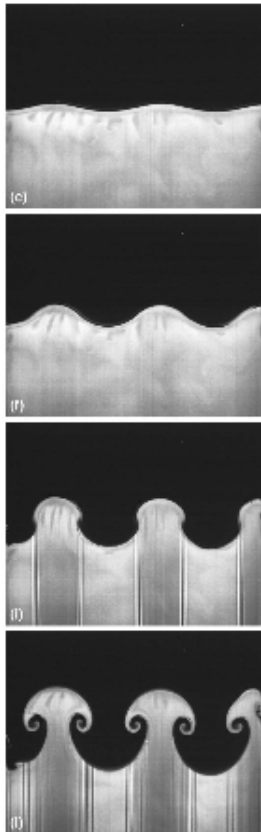
Results Interpretation



Challenges: Interfacial Instabilities

❑ Rayleigh Taylor Instability:

Lighter Fluids acceleration into heavier fluid results in **Rayleigh Taylor Instability**, Rayleigh (1882), Taylor (1950)



Time



❑ Saffman-Taylor Instability:

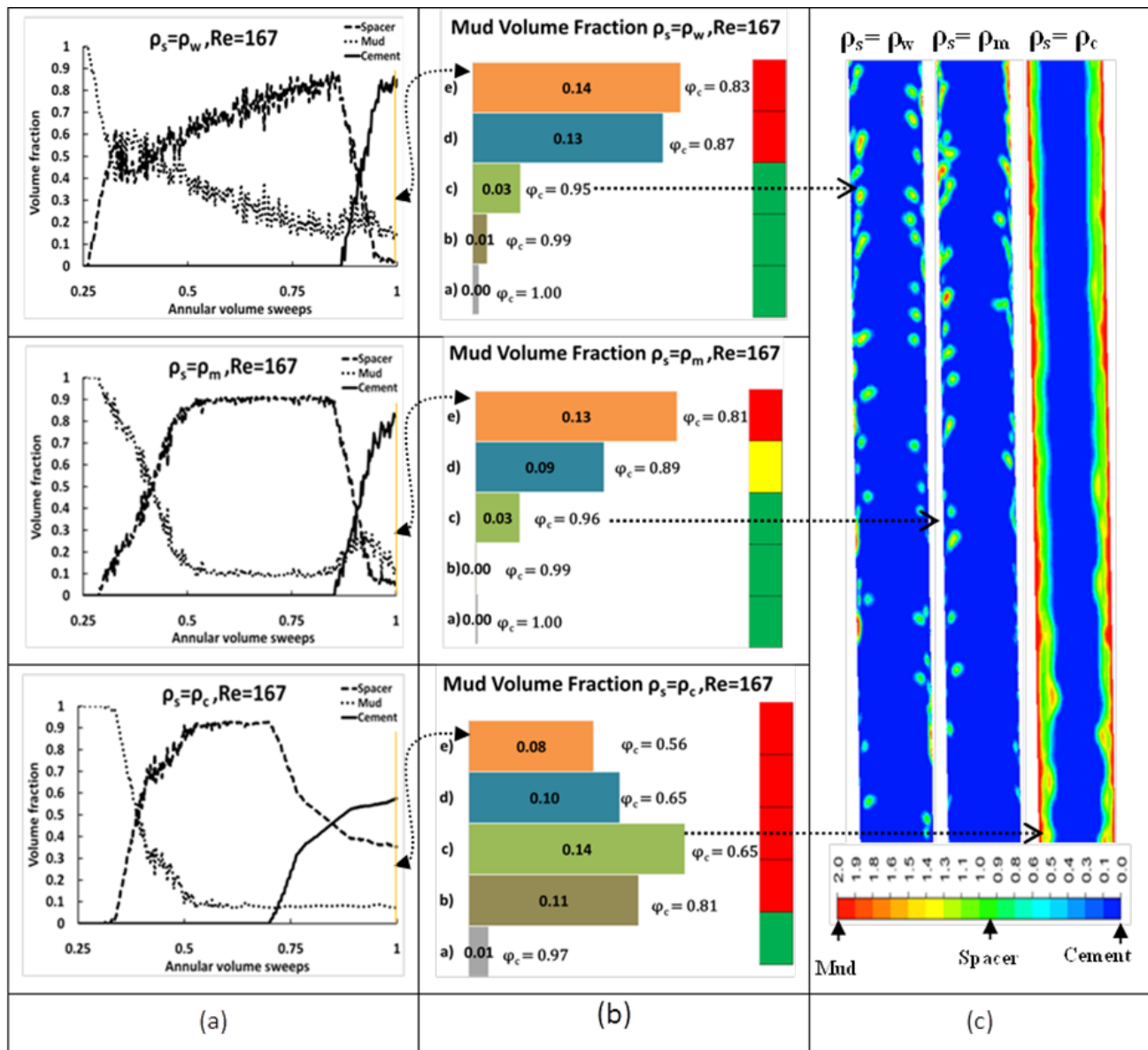
Displacement of more viscous fluid by less viscous results in **Saffman-Taylor instability**, Saffman and Taylor (1958)



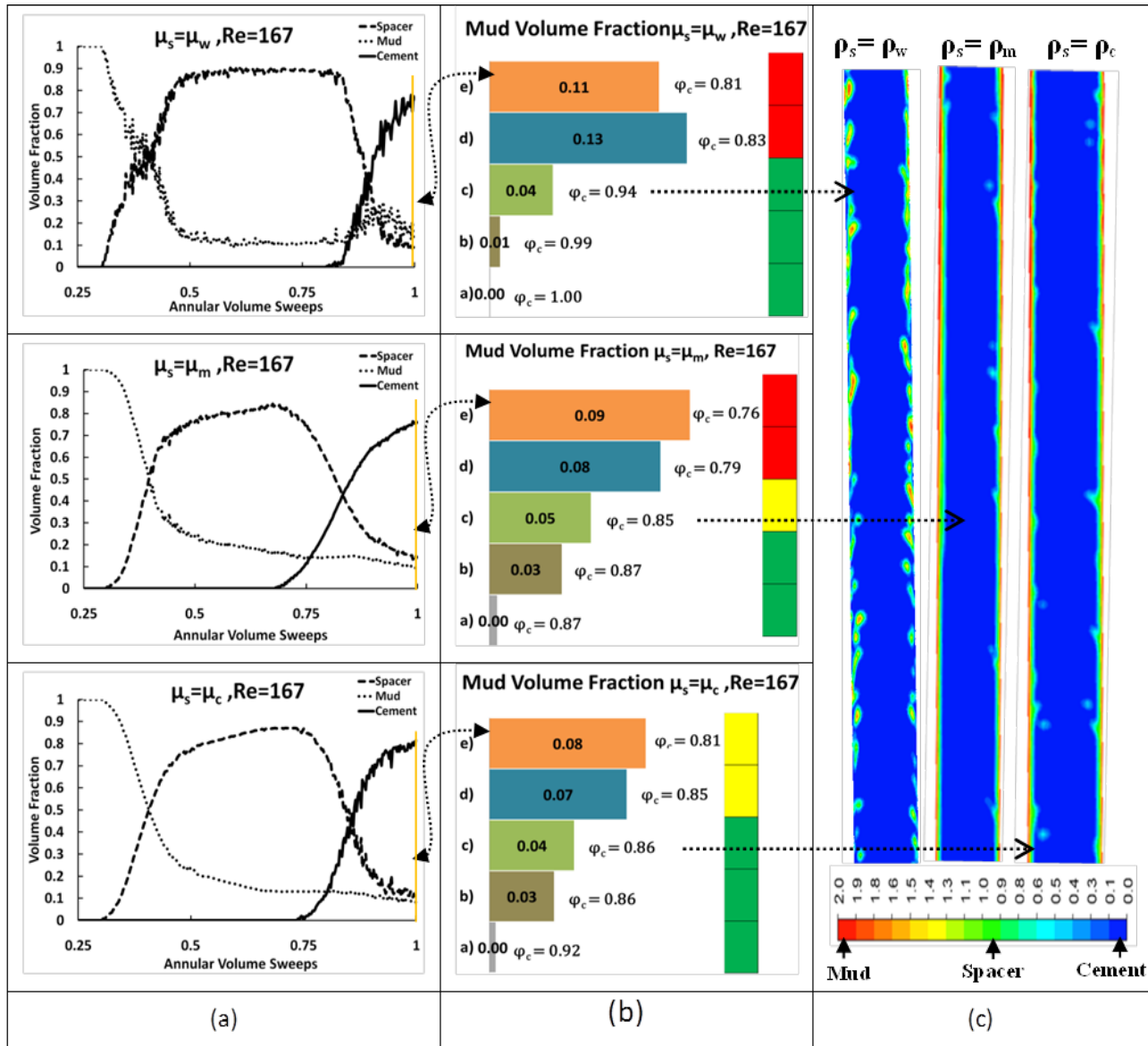
http://www.efluids.com/efluids/gallery/gallery_pages/JH03/text.jsp

Prof. J. Hertzberg

Density Variations



Viscosity Variation



CFD Based Correlation

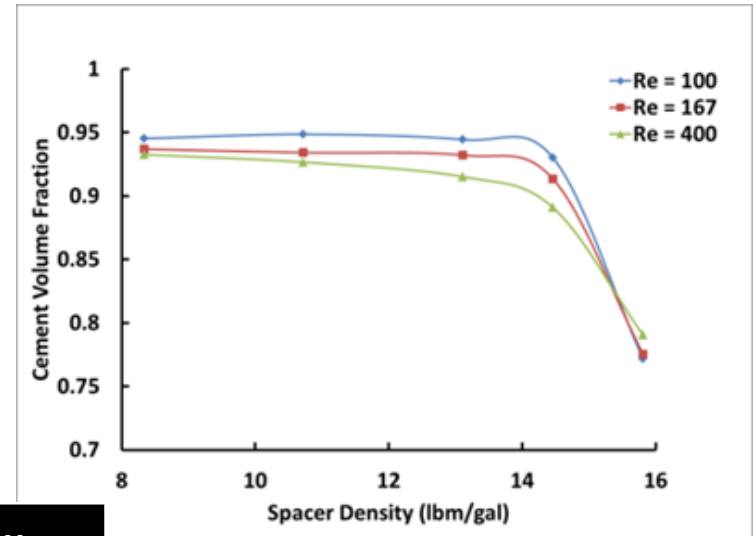
Due to the nature of fluid being used the correlation is expected to be of the form of power law

$$\varphi_c = \gamma \rho^a \mu^b Re^c \quad (1)$$

Where φ_c is the cement volume fraction, γ is a constant multiplier,

$$\rho = \frac{\rho_s}{\sqrt{\rho_m * \rho_c}}, \mu = \frac{\mu_s}{\sqrt{\mu_m * \mu_c}}$$

Re is the Reynolds number and a, b, c are constants.



Variable	a	b	c	γ_1	γ_2	γ_3
Value	-0.0113	-0.0376	-0.0304	0.87334	0.73899	0.91210

$$\varphi_c = 0.86705 * \rho^{-0.0113} * \mu^{-0.0376} * Re^{-0.0304} \quad (For \rho_s < \rho_c, \mu_s < \mu_c) \quad (2)$$

$$\varphi_c = 0.74692 * \rho^{-0.0113} * \mu^{-0.0376} * Re^{-0.0304} \quad (For \rho_s = \rho_c, \mu_s = \mu_w) \quad (3)$$

$$\varphi_c = 0.91176 * \rho^{-0.0113} * \mu^{-0.0376} * Re^{-0.0304} \quad (For \mu_s = \mu_c, \rho_s = (\frac{\rho_c + \rho_m}{2})) \quad (4)$$



The value of R^2 was found to be 0.975, which shows a reasonable fit.

Concluding Remarks

- If cement and mud are compatible to each other than the fresh water will be the most effective means of displacing mud and detaching the adhered mud layer to walls
- If cement and mud are incompatible than a spacer with density equal to that of mud and viscosity of fresh water will be most effective
- For vertical well the final cement fraction slightly decreases with increasing displacement rate for spacer having density less than cement, while for the spacer density equal to cement the opposite is true
- CFD offers good tools to model complex fluid displacement processes, more complexities can be incorporated in future studies like variable bore hole, effect of temperature, modeling for the entire length using moving meshes etc.
- Other simulations (not presented here) – Horizontal wellbores, Varying rheology, Varying displacement rates.



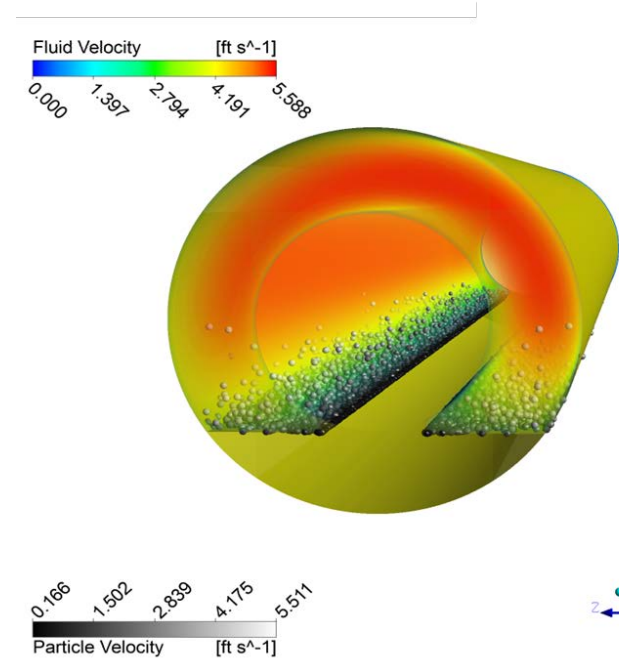
Future Directions (Component scale applications)

- Cement job in long horizontal wellbores
- Fluid displacement instabilities during 180° turn at the casing end
- Modeling foamed cement displacement (in contrast to H-B rheology)
- Multiphase turbulent flow simulations in petroleum engineering field equipment such as slotted liners, gravel packs etc.
- ... and couple heat transfer, phase change etc. to improve the engineering design



Discrete Phase Simulations of Cuttings Transport in Highly Deviated Wellbores

- Physics of cuttings transport
- Review: Previous modeling approaches
- Computational model description, boundary conditions and simulation procedures
- Results – verification & validation, cuttings bed height & moving bed velocity estimation, parametric study
- Discussions
- Conclusions and future directions

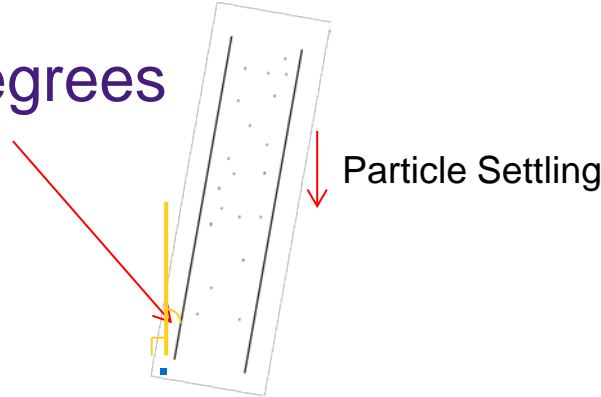


Cuttings Transport Mechanisms and Issues at Different Wellbore Inclinations

Main
Transport
Mechanism:
Suspension

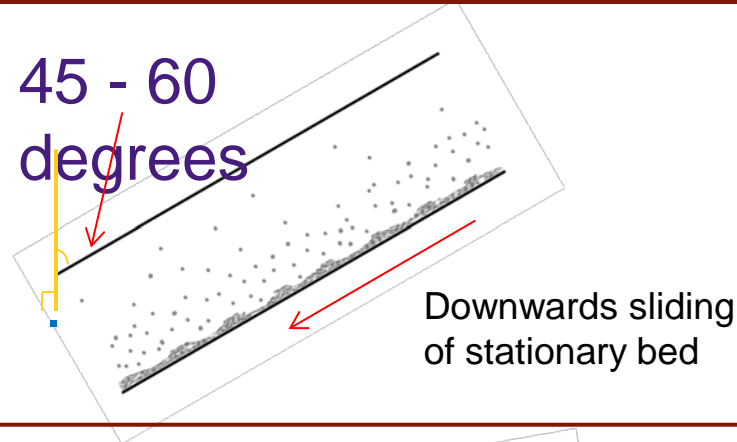
0 - 45 degrees

Vertical – Near
Vertical Wellbores



Critical Inclinations

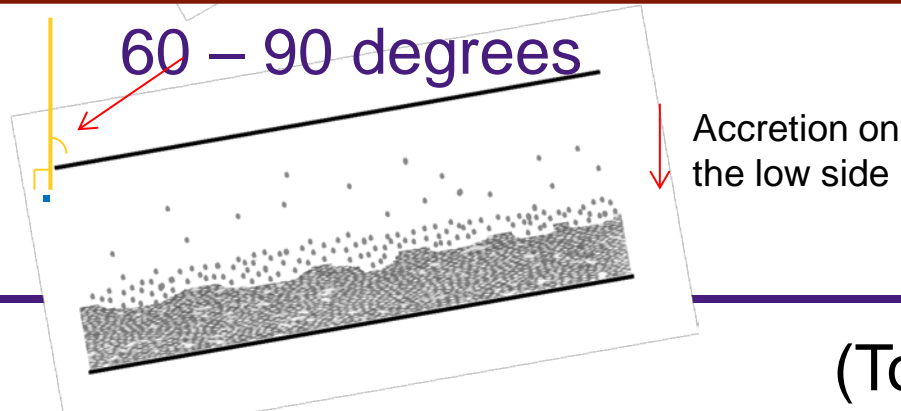
45 - 60
degrees



*Suspension
& Moving
Bed*

Horizontal – Near
Horizontal Wellbores

60 – 90 degrees



*Suspension &
Moving Bed*



(Tomren et al, 1986)

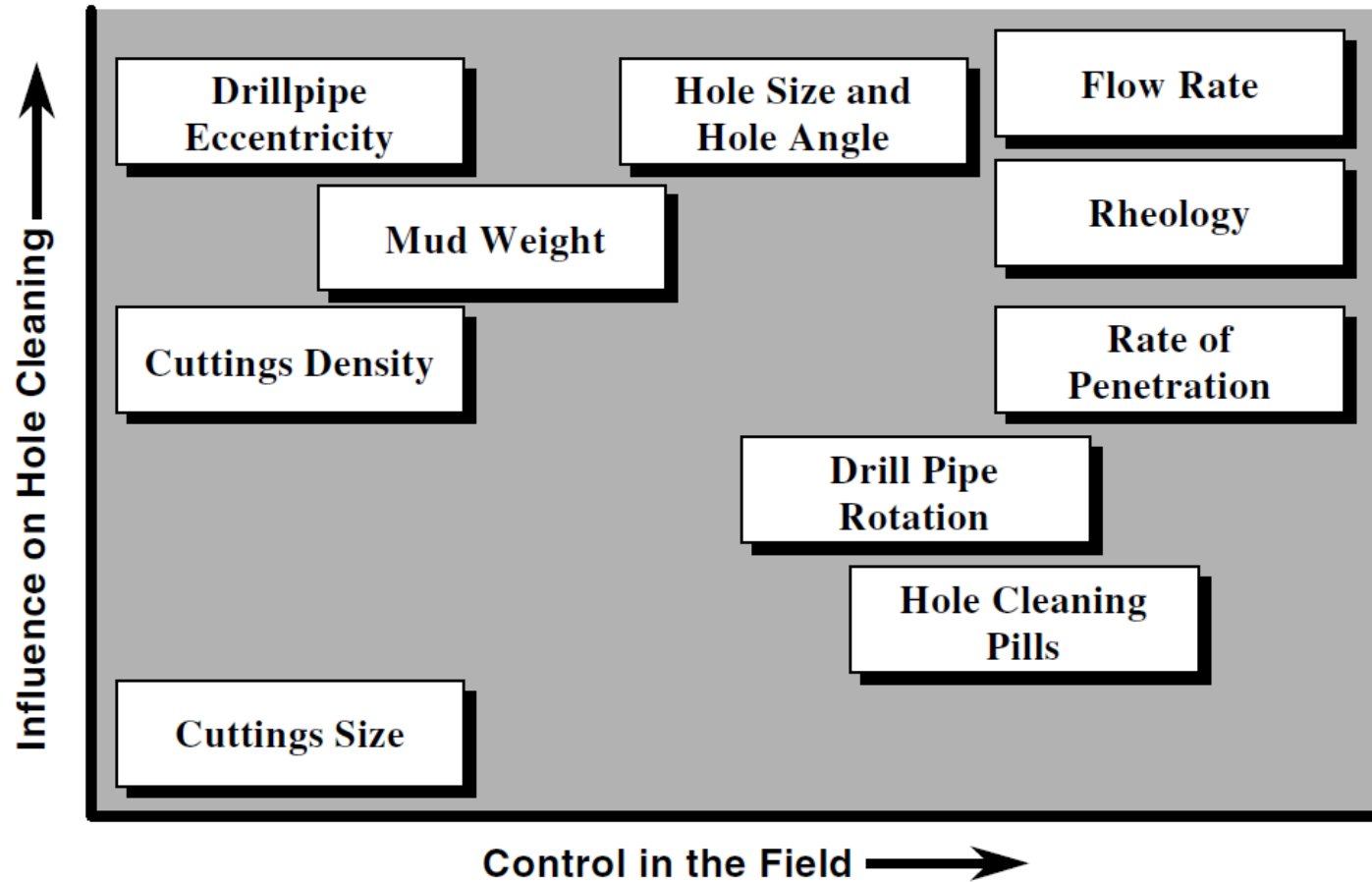
Risks of High Solids Concentration in the Wellbore

- High torque and drag
- Poor hole condition
- Stuck pipe
- Difficulty in running and cementing casing



(Brown et al., 1989)

Parameters involved in Cuttings Transport Process



A cuttings transport model should predict the following:

- Maximum bed height *for*:
 - Optimizing drilling parameters for adequate wellbore cleaning.
- Particle velocities *for*:
 - Circulation time estimation
 - Solids concentration control
- Frictional pressure losses due to solids concentration



Numerical Setup Summary

A 3D model couples main fluid mass and momentum conservation with:

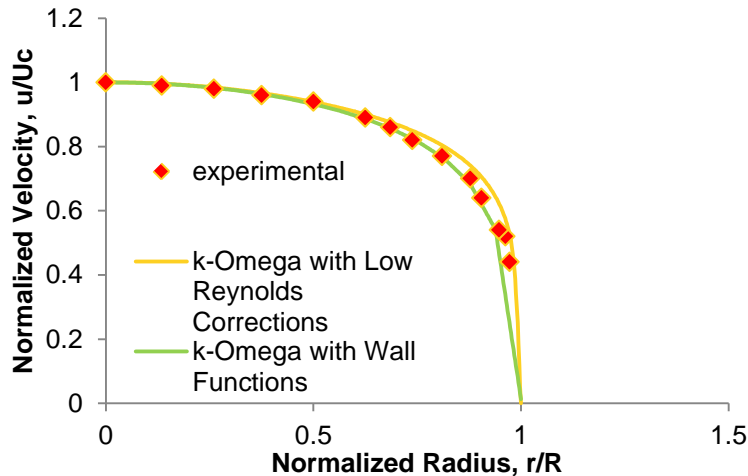
- Shear Stress Transport (SST) k-Omega Turbulence Closure
- Discrete Phase Model

Includes:

- Non – Newtonian Rheology
- Wall Roughness for Fluid Flow (Modified Law of the Wall)
- Turbulent Dispersion of Particles (Random Walk Model)
- Non spherical particles (Modified drag coefficient)

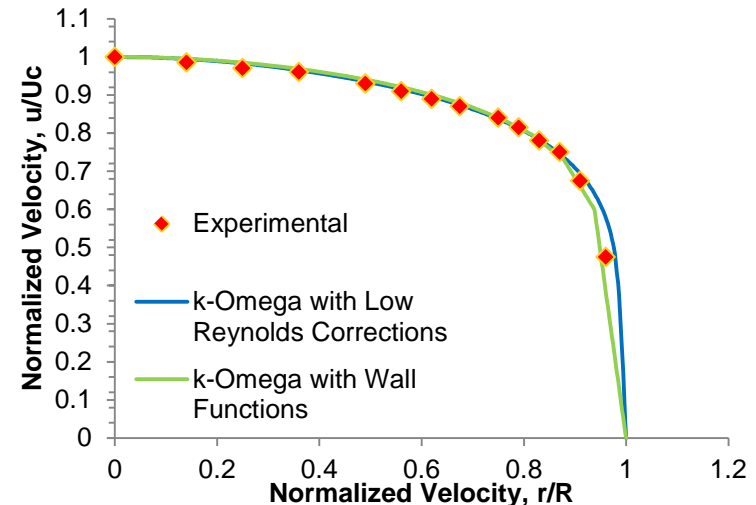


Turbulent Flow of Non – Newtonian Fluids



Comparison of experimental data from Pereira and Pinho with CFD results. Experimental Setup:

- Pipe Radius: 26 mm
 - Fluid: Water with 0.4% Tylose
 - Rheology: Carreau Model
- λ (s) = 0.0208, μ_0 = 0.00407, n = 0.725
 Mean Velocity: 5.59 m/s



Comparison of experimental data from Piho and Whitelaw with CFD results. Experimental Setup:

- Pipe Radius: 25.4 mm
 - Fluid: Water with 0.4% CMC
 - Rheology: Power Law
- $k=0.447$, $n=0.56$
 Mean Velocity: 4.8 m/s

Discrete Phase Model

- Governing Equation:

$$\frac{\partial u_p}{\partial t} = \underbrace{F_D(u - u_p)}_{\text{Drag Force Term}} + \underbrace{\frac{g_x(\rho_p - \rho)}{\rho_p}}_{\text{Buoyancy Term}} + F_x$$

Includes non-spherical drag coefficient

Additional forces: Pressure Gradient Force, Virtual Mass force (Force needed to accelerate the surrounding fluid)

Estimation of Cuttings Bed Height

For an accretion/erosion model following mechanisms should be known:

1. How does particles lose momentum upon impact?
2. How does particles accrete and form a bed?



Particle-Fluid Interaction Forces

Forces	Correlations	References
Drag force	<p>For an isolated particle moving through a gas, $\mathbf{F}_d = C_d \pi \rho_f d_p^2 \mathbf{u} - \mathbf{v} (\mathbf{u} - \mathbf{v}) / 8$ Effect of surrounding particles is described by a voidage function, $f(\varepsilon_f)$: $\mathbf{F}_d = f(\varepsilon_f) C_d \pi \rho_f d_p^2 \mathbf{u} - \mathbf{v} (\mathbf{u} - \mathbf{v}) / 8$ $C_d = 24(1 + 0.15 Re_p^{0.687}) / Re_p$ ($Re_p < 1000$) $C_d = 0.44$ ($Re_p > 1000$) $Re_p = \rho_f d_p \varepsilon_f \mathbf{u} - \mathbf{v} / \mu_f$</p> <p>$\mathbf{F}_d = \beta_{pf} (\mathbf{u} - \mathbf{v}) / \rho_f$ $\beta_{pf} = 150 \frac{(1 - \varepsilon_f)^2}{\varepsilon_f} \frac{\mu_f}{(\phi_p d_p)^2} + 1.75(1 - \varepsilon_f) \frac{\rho_f}{\phi_p d_p} \mathbf{u} - \mathbf{v}$ ($\varepsilon_f \leq 0.8$) $\beta_{pf} = \frac{3}{4} C_d \frac{ \mathbf{u} - \mathbf{v} \rho_f (1 - \varepsilon_f)}{d_p} \varepsilon_f^{-2.7}$ ($\varepsilon_f > 0.8$)</p> <p>$f(\varepsilon_f) = \varepsilon_f^{-(\alpha+1)}$ $\alpha = 3.7 - 0.65 \exp[-(1.5 - \log Re_p)^2 / 2]$</p> <p>$\mathbf{F} = \mathbf{F}_0(\phi) + \mathbf{F}_1(\phi) Re_p^2$ ($Re_p < 20$) $\mathbf{F} = \mathbf{F}_0(\phi) + \mathbf{F}_3(\phi) Re_p^2$ ($Re_p > 20$) $\mathbf{F}_0(\phi) = \frac{1+3(\phi/2)^{1/2}+(135/64)\phi \ln \phi + 16.14\phi}{1+0.681\phi-8.48\phi^2+8.16\phi^3}$ ($\phi < 0.4$) $\mathbf{F}_0(\phi) = 10\phi / (1 - \phi)^3$ ($\phi > 0.4$) $\mathbf{F}_1(\phi) = 0.110 + 5.10 \times 10^{-4} e^{11.6\phi}$ $\mathbf{F}_3(\phi) = 0.0673 + 0.212\phi + 0.0232(1 - \phi)^5$</p>	<p>Ergun (1952), and Wen and Yu (1966)</p> <p>Di Felice (1994)</p> <p>Koch and Sangani (1999), and Koch and Hill (2001)</p>
Pressure gradient force	<p>$\mathbf{F}_p = -V_p d p / d x = -V_p (\rho_f \mathbf{g} + \rho_f \mathbf{u} d \mathbf{u} / d x)$ It is of general validity and all relevant contributions are included when $d p / d x$ is evaluated from the fluid equation of motion.</p>	Anderson and Jackson (1967)
Virtual mass force	<p>$\mathbf{F}_{Vm} = C_{vm} \rho_f V_p (\dot{\mathbf{u}} - \dot{\mathbf{v}}) / 2$ $C_{Vm} = 2.1 - 0.132 / (0.12 + A_c^2)$ $A_c = (\mathbf{u} - \mathbf{v})^2 / (d_p d(\mathbf{u} - \mathbf{v}) / d t)$</p>	Odar and Hamilton (1964), and Odar (1966)
Basset force	<p>$\mathbf{F}_{Basset} = \frac{3}{2} d_p^2 \sqrt{\pi \rho_f \mu_f} \left[\int_0^t \frac{(\dot{\mathbf{u}} - \dot{\mathbf{v}})}{\sqrt{t - t'}} dt' + \frac{(\mathbf{u} - \mathbf{v})_0}{\sqrt{t}} \right]$ where $(\mathbf{u} - \mathbf{v})_0$ is the initial velocity difference</p>	Reeks and Mckee (1984), and Mei et al. (1991)
Saffman force	<p>$\mathbf{F}_{Saff} = 1.61 d_p^2 (\mu_f \rho_f)^{1/2} \boldsymbol{\omega}_c ^{-1/2} [(\mathbf{u} - \mathbf{v}) \times \boldsymbol{\omega}_c]$ $\boldsymbol{\omega}_c = \nabla \times \mathbf{u}$</p>	Saffman (1965, 1968)
Magnus force	<p>$\mathbf{F}_{Mag} = \frac{\pi}{8} d_p^2 \rho_f \left[\left(\frac{1}{2} \nabla \times \mathbf{u} - \boldsymbol{\omega}_d \right) \times (\mathbf{u} - \mathbf{v}) \right]$ where $\frac{1}{2} \nabla \times \mathbf{u}$ is the local fluid rotation and $\boldsymbol{\omega}_d$ is the particle rotation. One notes that the lift would be zero if the particle rotation is equal to the location rotation of the fluid</p>	Rubinow and Keller (1961)

Hypotheses for Equilibrium Cuttings Bed Height

Particle-Wall Interactions

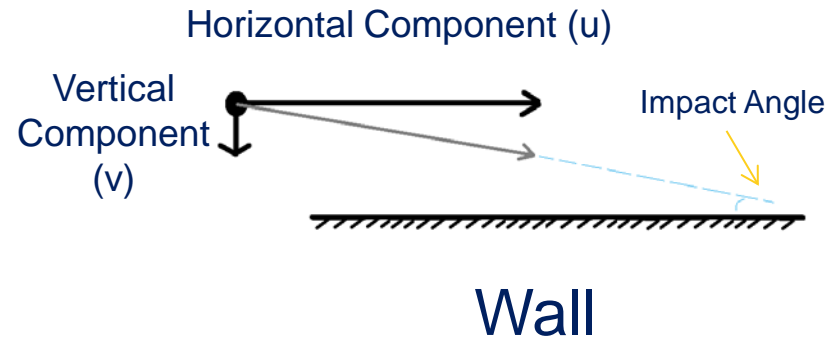
Hypotheses based on experimental observations of particle-wall collisions:

With increasing flow rate and decreasing accumulation rate, the following should be observed:

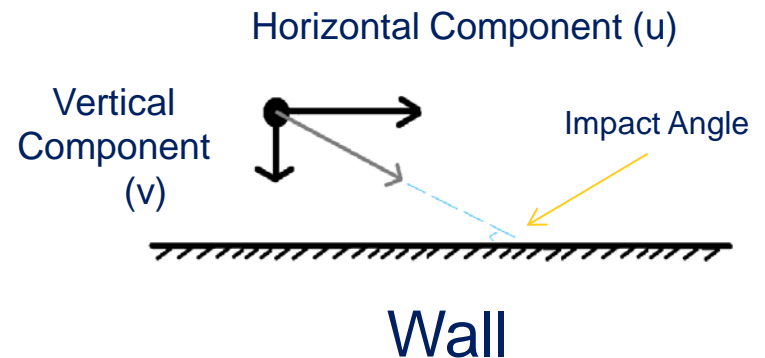
1. Increase in P-W IMPACT VELOCITY
2. Decrease in TOTAL NUMBER OF P-W COLLISIONS
3. Decrease in MAXIMUM P-W IMPACT ANGLE
4. Increase in DISTANCE COVERED IN SUSPENSION



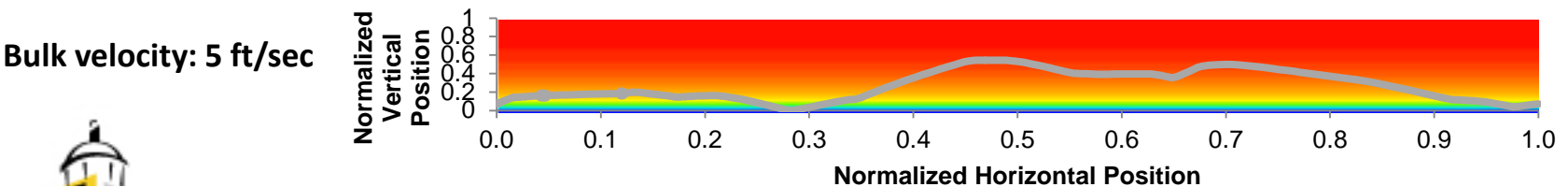
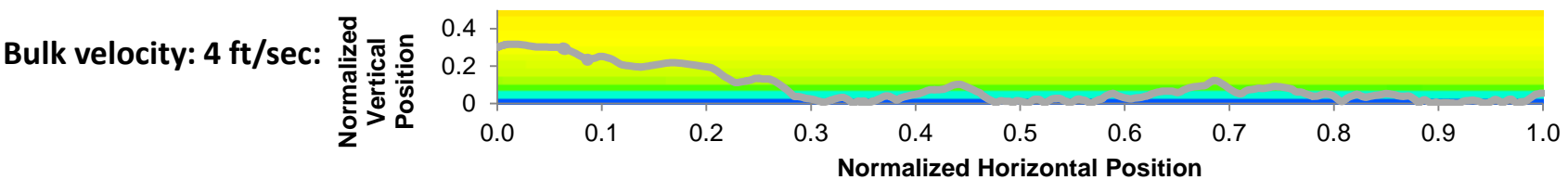
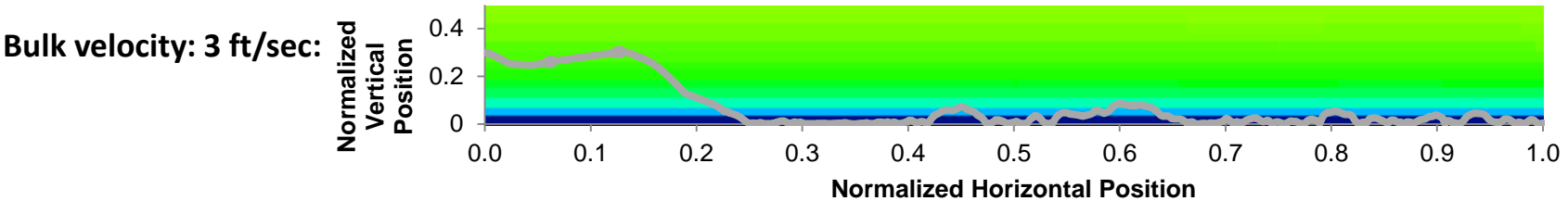
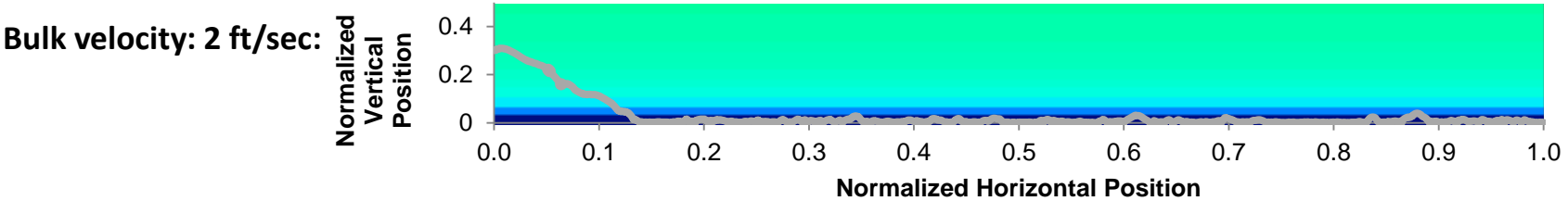
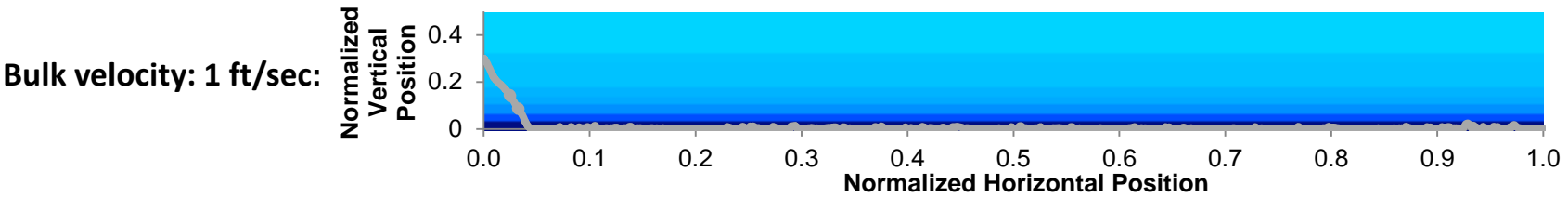
SMALL IMPACT ANGLE:



LARGE IMPACT ANGLE:

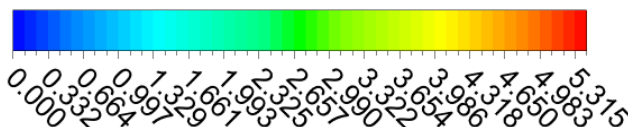


Particle – Wall Collision Analysis

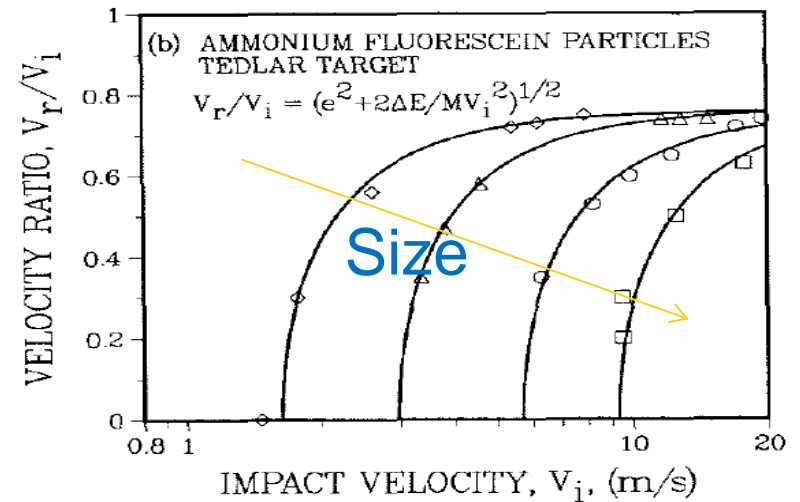
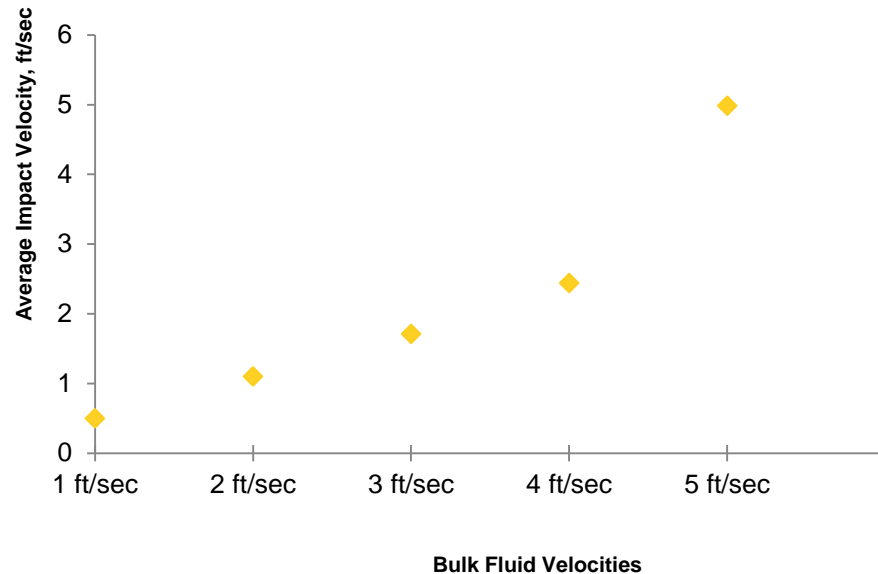


Fluid Velocity

[ft s⁻¹]



Particle Track Analysis: P – W Impact Velocities



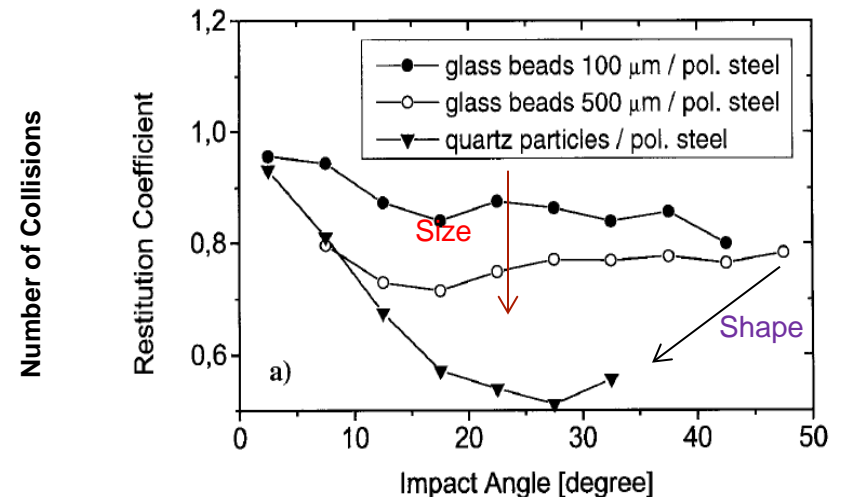
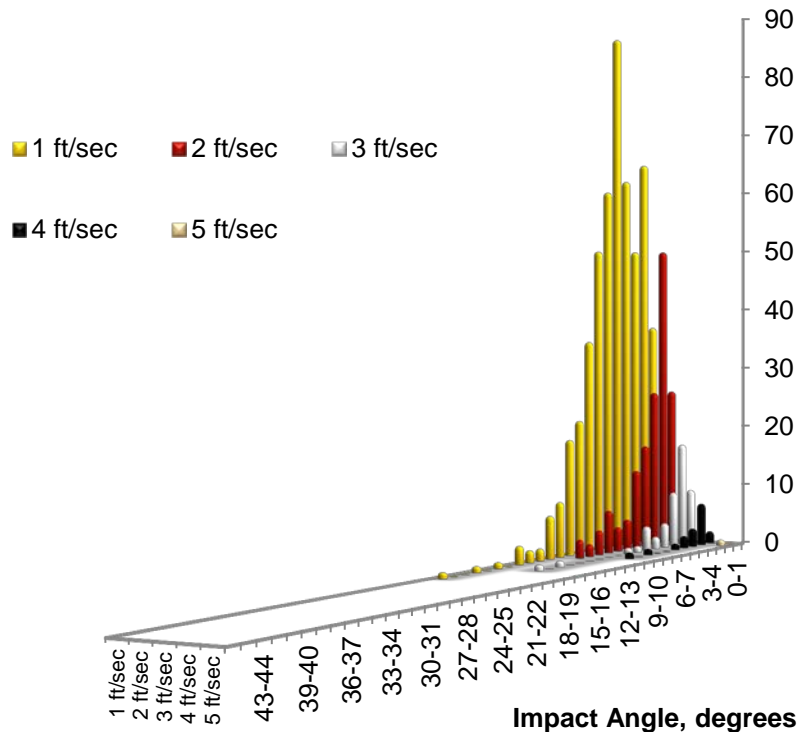
P-W Impact velocities at different bulk fluid velocities.

IMPACT VELOCITY increases with increasing flow rate



Particle Track Analysis

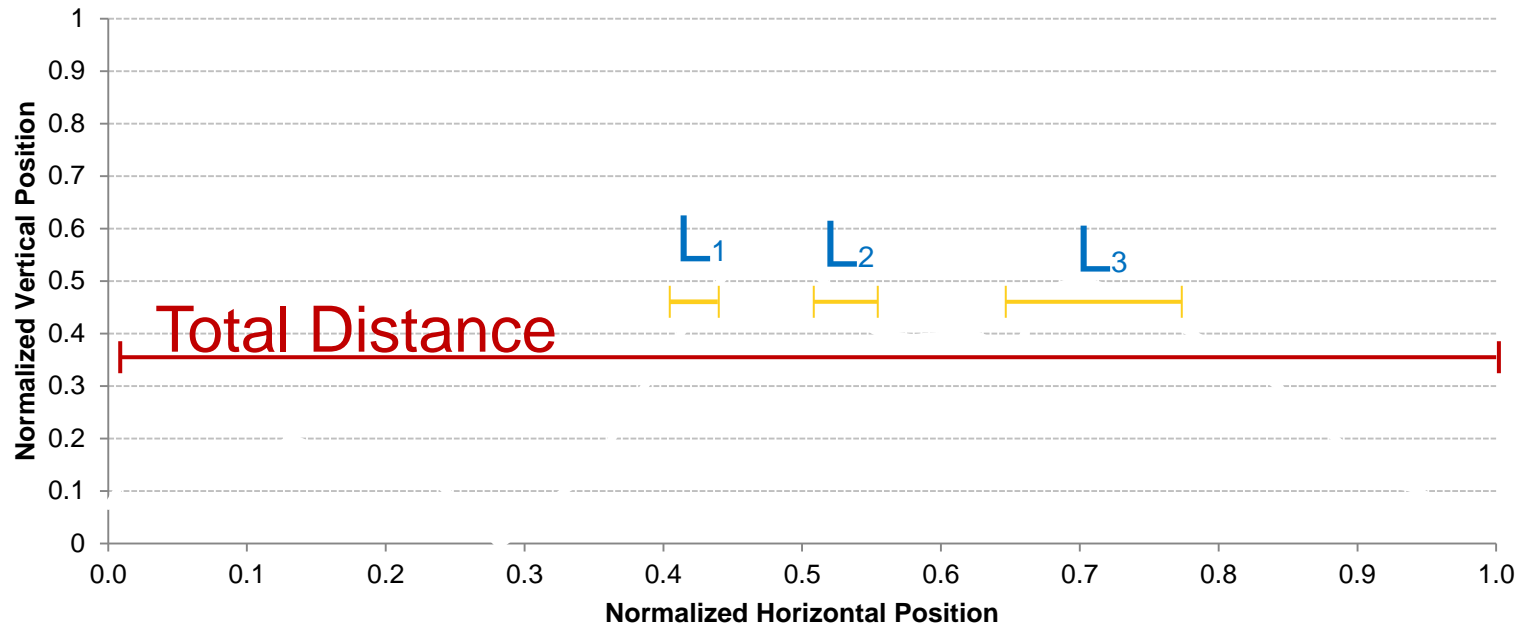
P – W Impact Angles



Number of collisions with different impact angles

- TOTAL NUMBER OF COLLISIONS decreases with increasing FLOW RATE
- MAXIMUM IMPACT ANGLE decreases with increasing FLOW RATE

Particle Track Analysis: Distance Covered in Suspension



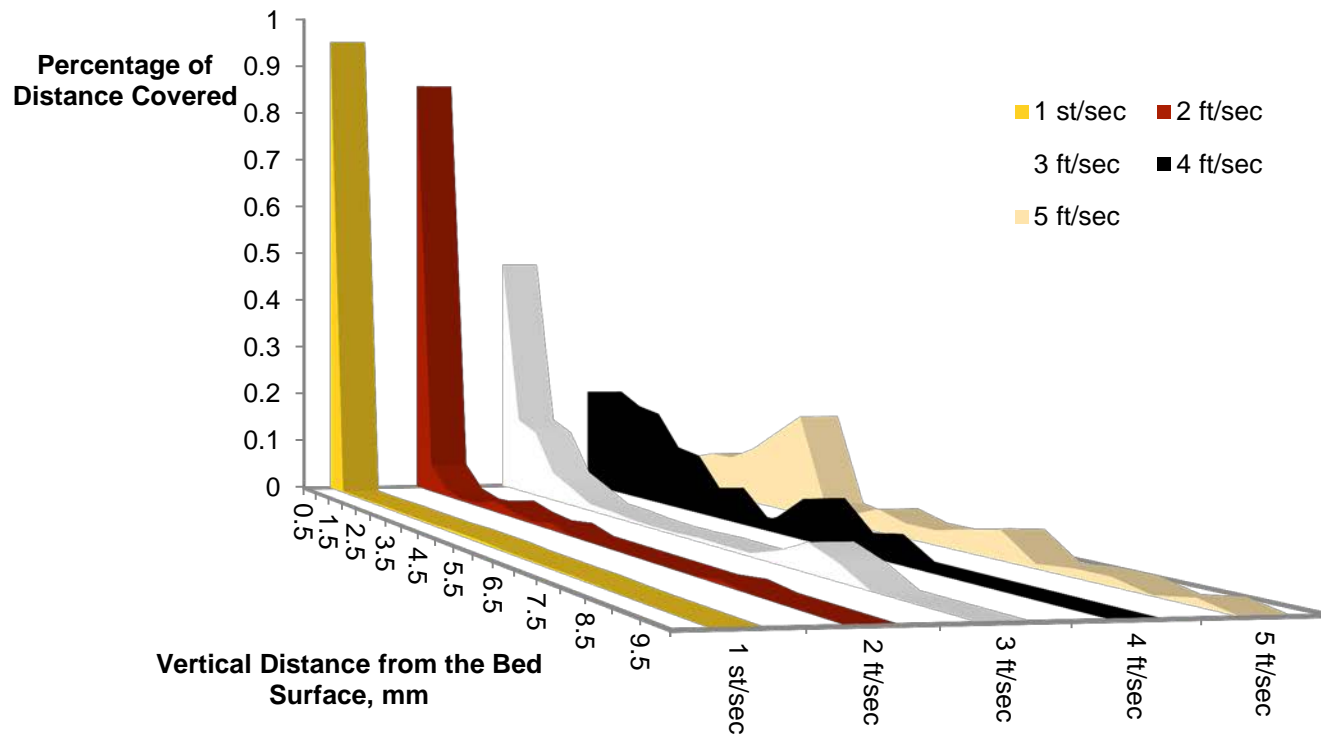
Example:

Percentage Horizontal distance covered between norm. vertical distances
0.4 and 0.5:

$$[L_1 + L_2 + L_3] / \text{Total Distance}$$

Particle Track Analysis

Distance Covered in Suspension



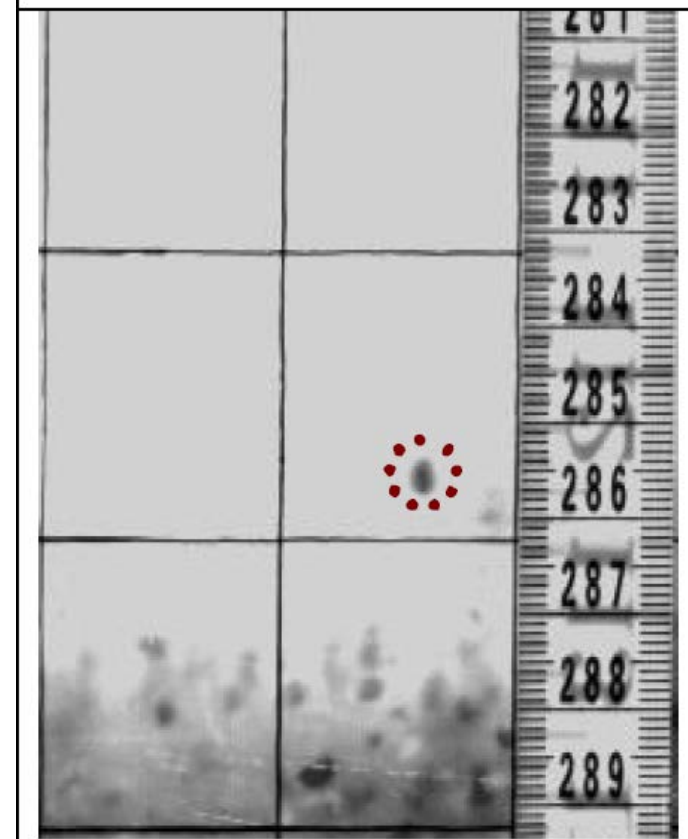
Experimental Test Matrix: (Garcia – Hernandez et al.)

Experimental Setup:

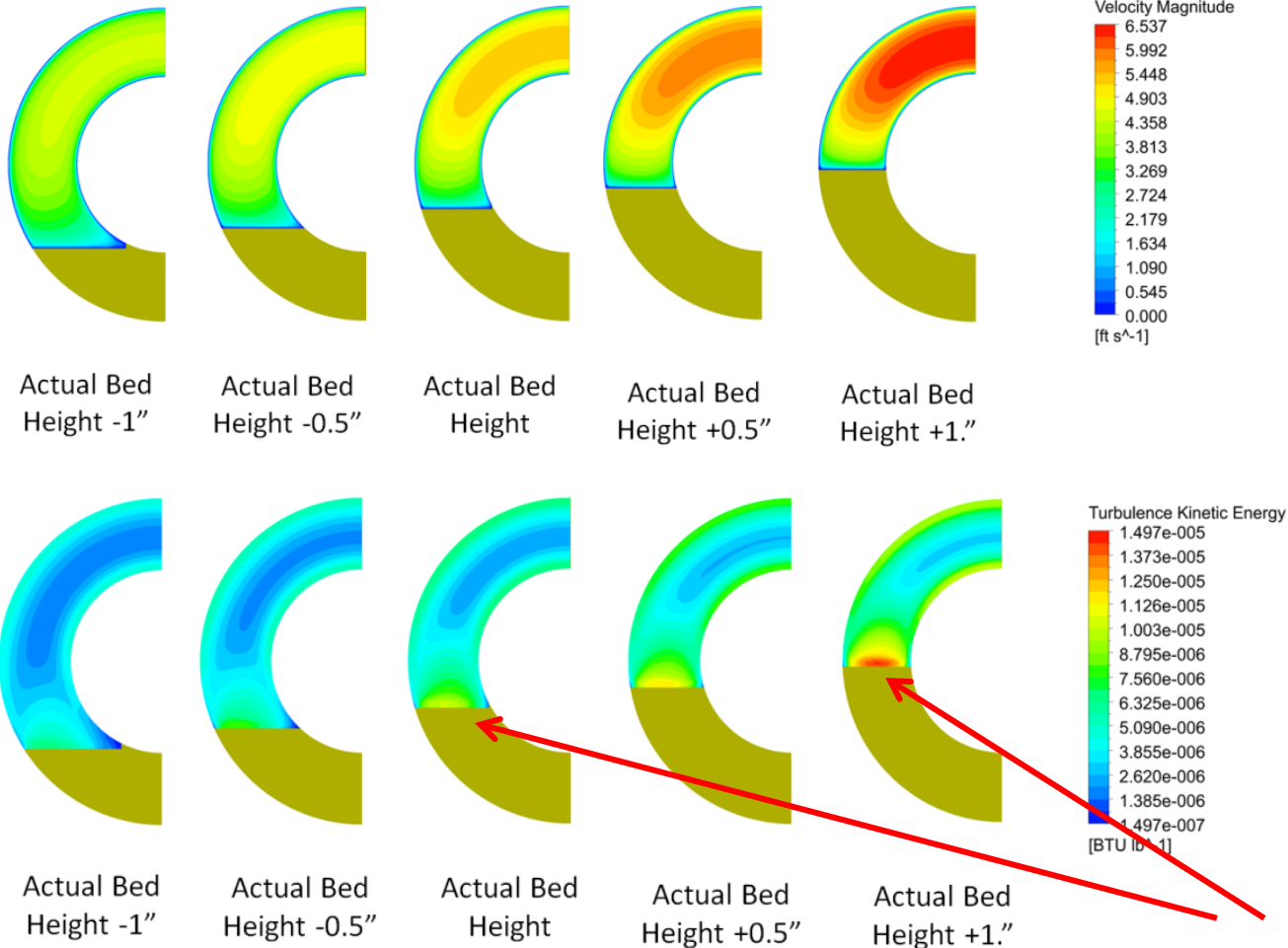
- Geometry: 8" x 4.5" concentric Annulus
- Carrier Fluid: Water
- Particles: Gravel
- Particle Size: 3 – 5 mm
- Particle Specific Gravity: 2.6

Experimental Procedure:

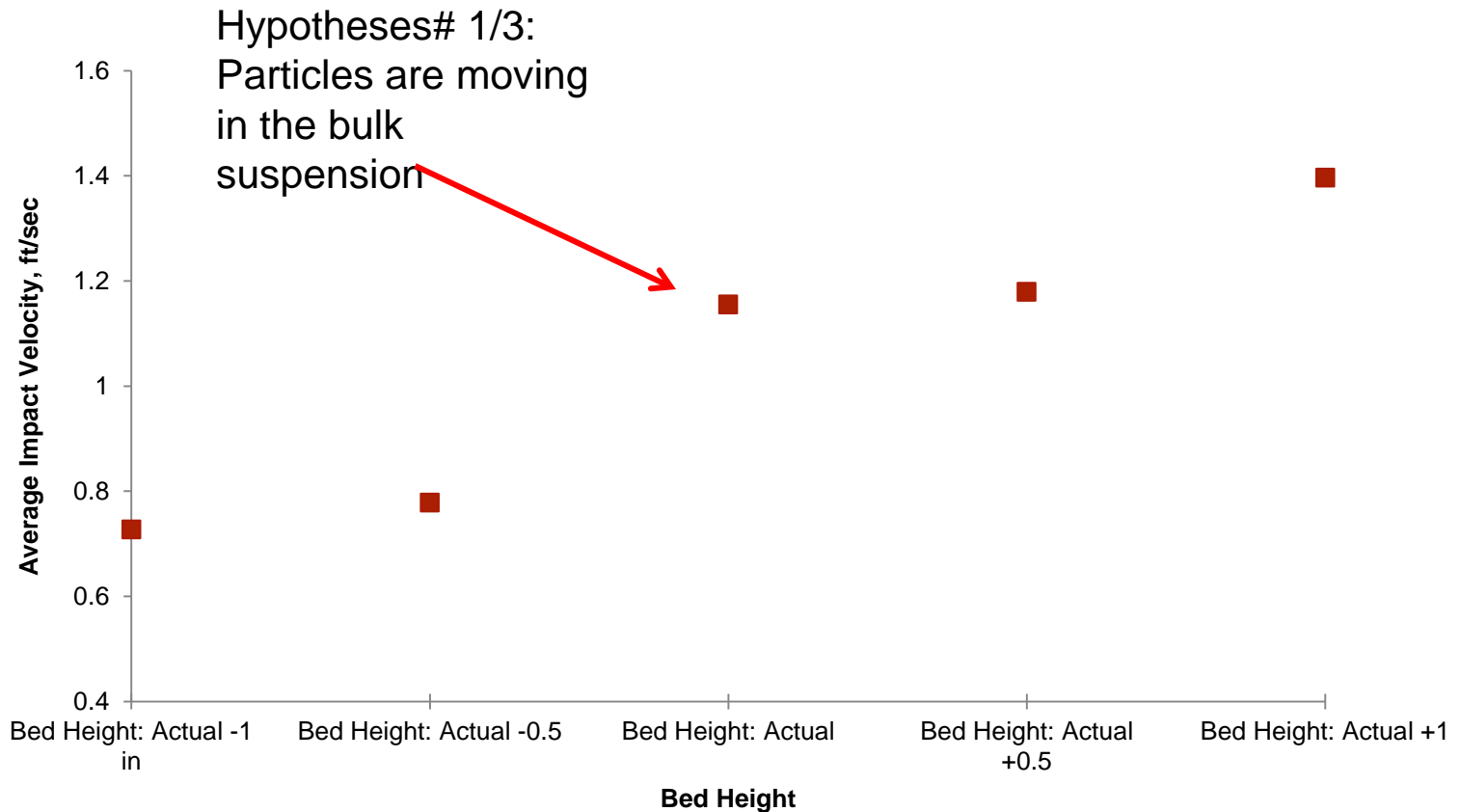
- After flow is stabilized (Periodic) solid particles are injected from one end of the flow loop.
- After the stationary bed reached an equilibrium (No change) bed heights are measured on different points.
- Bulk velocities are calculated by dividing the flow rate to the decreased flow area by the bed.
- Velocities of marked particles are measured by image velocimetry method.
- Particle velocities are averaged until no change in the average.



300 gpm – 70 degrees Wellbore Inclination



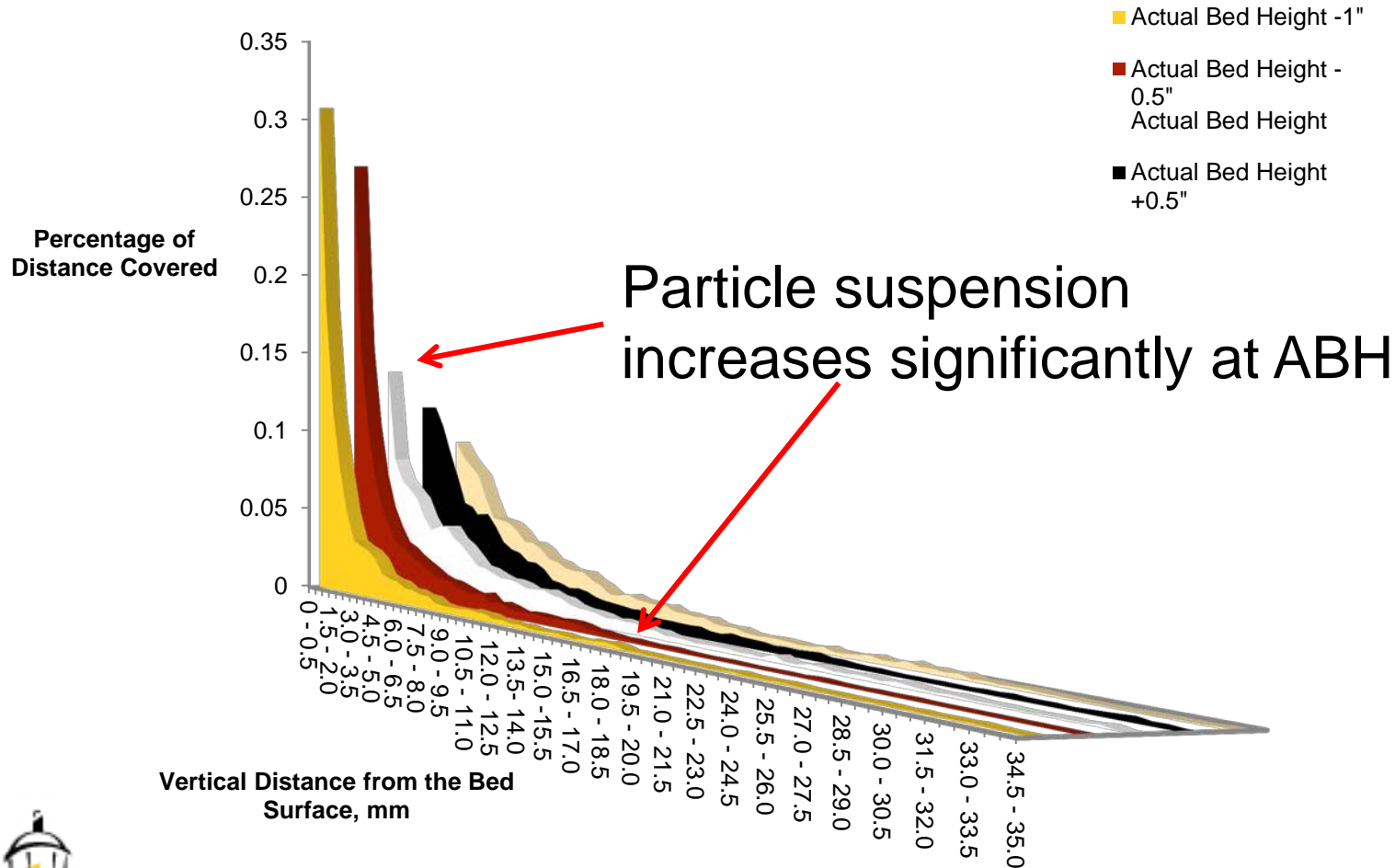
300 gpm – 70 degrees Wellbore Inclination



Averaged impact velocities

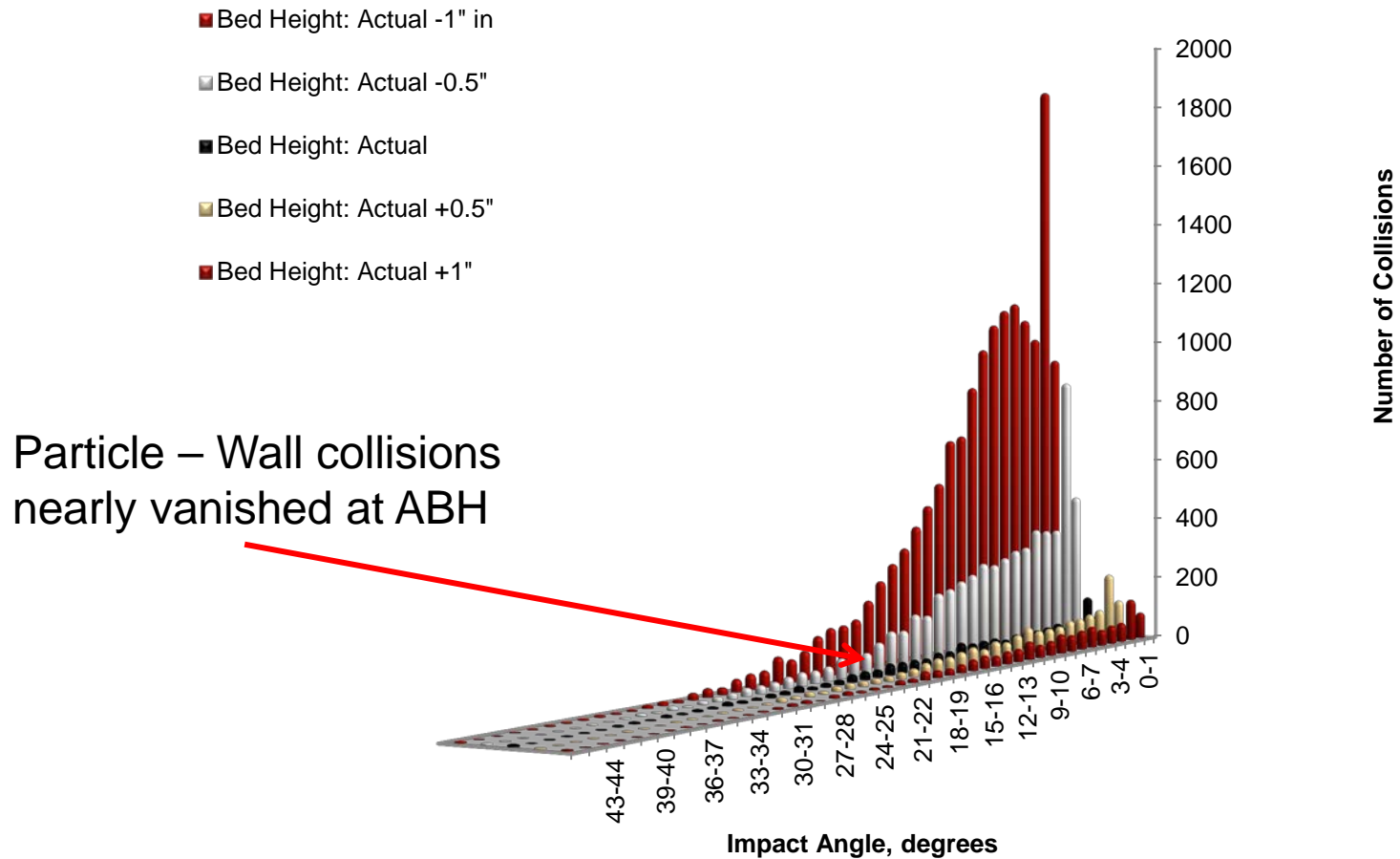
300 gpm – 70 degrees Wellbore Inclination

Distance Covered in Suspension



300 gpm – 70 degrees Wellbore Inclination

Particle – Wall Collisions

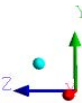
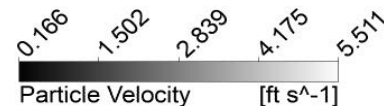
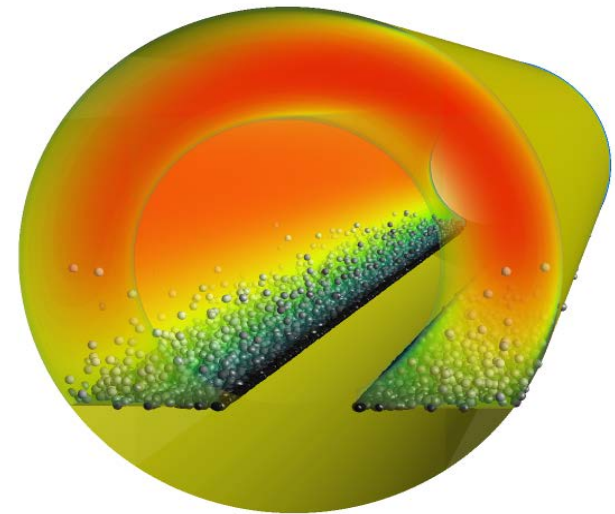
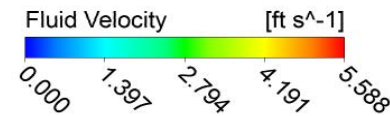


Moving Bed Velocity Validation

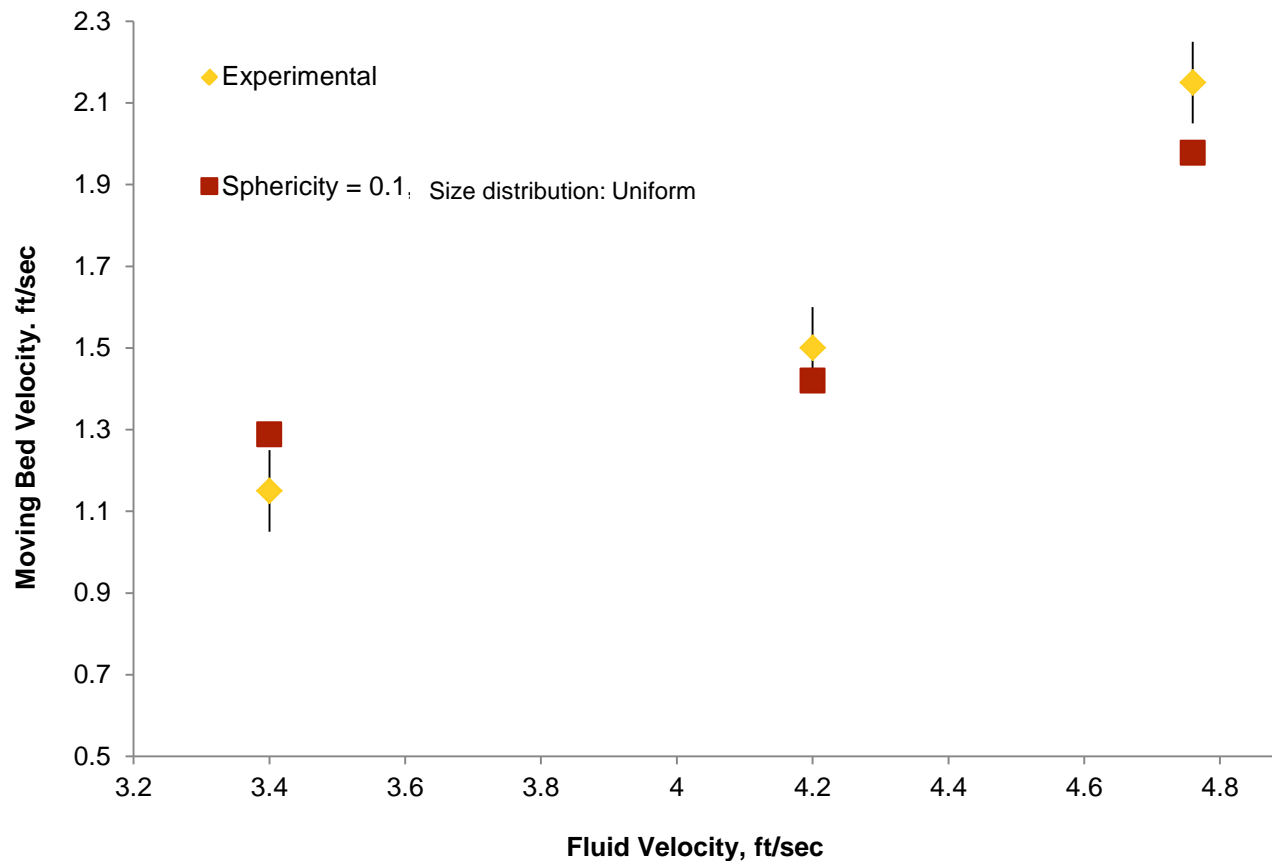
Unsteady Particle Tracking: Particles are injected and particle paths are calculated at every time step.

Assumptions:

1. Sphericity is uniform and has the value 0.1 for all particles
2. Stationary bed height reached equilibrium, flow shear compensates for momentum loss due to particle-wall collisions.



Moving Bed Velocity Validation



Model Limitations

- DPM and SST $k-\omega$ turbulence model are coupled in a one way fashion in which the effects of particle motion on flow field is neglected.

Model is not responsive to solids loading (or ROP). The effects of solids on frictional pressure losses are discarded.

- Particle – particle interactions are also neglected assuming solids concentration is low enough.

However, P-P interaction forces can be important in cases where accurate particle shape information is available.

Model Limitations

- Suspension levels in cases with inner pipe rotation were not as high as described in experimental works. Orbital movement of the pipe and vibrations should also have K. E. contributions to the flow.
- Particle size distribution is found to have negligible effect on the moving bed velocity. It can be influential in wider ranges.
- Two-equation turbulence models can not capture transient regimes where molecular viscosity and eddy viscosity can be equally effective.



Concluding Remarks

- Accurate prediction of velocity profiles of non-Newtonian fluids flowing in turbulent regime.
- Accurate prediction of stationary bed heights in horizontal wellbores with different flow rates, inclined wellbores and wellbores with inner pipe rotations. The effects of wellbore inclination and inner pipe rotation are in agreement with experimental observations through validation.
- Accurate prediction of average moving bed velocity.
- Qualitative sensitivity studies are conducted for fluid density, rheology, particle sphericity and size distribution and inner pipe rotation speed (Not presented here).



Future Directions (Cuttings Transport)

- Full wellbore flow path
- Coupling of particle-wall interactions (DEM)
- Morphology of cuttings bed

Questions

